

An efficient and optimal adsorptive removal of glufosinate ammonium from wastewater using carbonized rice husk-clay blend briquettes

Emmanuel Amuntse Yerima^{1*}, Sheba P. Maaji¹, Fatuma C. Samuel-Okey², David Abutu³, Shem Afyenaku¹, Danladi Mudwa¹, Amani D. Haruna³, Samuel Audu¹

¹ Department of Chemistry, Federal University Wukari, PMB 1020, Taraba State, Nigeria

² Department of Integrated Science, Federal University of Education, Zaria, Nigeria

³ Department of Chemical Engineering, Faculty of Engineering, Federal University Wukari, PMB 1020, Taraba State, Nigeria

* Corresponding author's e-mail: yerimaemmanuel@yahoo.com

ABSTRACT

The persistence of glufosinate ammonium in agricultural runoff poses serious environmental and public health risks, necessitating the development of low-cost and sustainable remediation strategies, since most of the existing solutions such as the advance oxidation and electro-sorption methods are quite expensive, requiring technical expertise to be implemented. This study investigated the adsorptive removal of glufosinate ammonium from wastewater using carbonized rice husk-clay blend briquettes, a valorized agricultural byproduct. Response Surface Methodology (RSM) version 13 of the design expert was employed to optimize key operational parameters, including pH, temperature, contact time, and adsorbent dose. The adsorbent was characterized pre- and post-adsorption using Fourier transform infrared spectroscopy (FTIR), energy dispersive x-ray spectroscopy (EDX), scanning electron microscopy (SEM), and transmission electron microscopy (TEM). The FTIR analysis revealed shifts in characteristic peaks associated with functional groups such as $-\text{OH}$, $-\text{C}\equiv\text{C}-$, $\text{C}-\text{H}$, and $\text{C}-\text{N}$, confirming active sites for adsorption. Likewise, the SEM and TEM images showed well-defined porous structures, which became saturated after adsorption, while EDX detected the presence of additional elements, such as Fe and Cu, introduced from the wastewater matrix. Under optimal conditions (pH 7.5, 20 °C, 1.25 g adsorbent dose, and 100 min contact time), a removal efficiency of 90% was achieved. The adsorption kinetics followed a pseudo-second-order model ($k = 0.09 \text{ min}^{-1}$), while the equilibrium data conformed to the Freundlich isotherm, indicating multilayer adsorption on a heterogeneous surface. These results demonstrate that rice husk-clay briquettes offer a promising, and sustainable solution for the efficient removal of glufosinate ammonium from contaminated water.

Keywords: Glufosinate ammonium, contaminated water, remediation, rice husk, clay.

INTRODUCTION

Wastewater is any water the quality of which has been negatively impacted by human activity and cannot be directly returned to the environment without causing environmental harm (Ugrina *et al.*, 2024). The ecological perspective emphasizes the impact of waste water on natural ecosystems under scoring the need for proper treatment to avoid environmental degradation. The applications of herbicides like finis, sweeps, and dragon

super which contain glufosinate ammonium as the active ingredient has drawn environmental concerns to scientist due to its toxicity. Glufosinate is a fast-acting herbicide with the IUPAC name: ammonium (3-amino-3-carboxypropyl) methyl phosphate ($\text{C}_5\text{H}_{15}\text{N}_2\text{O}_4\text{P}$); It was initially identified as a natural product and is now the sole herbicide that targets glutamine synthetase (Takano and Dayan, 2020). Glufosinate ammonium has high solubility in water and can readily leach into surface and groundwater (Johnson, 2020) (Figure 1).

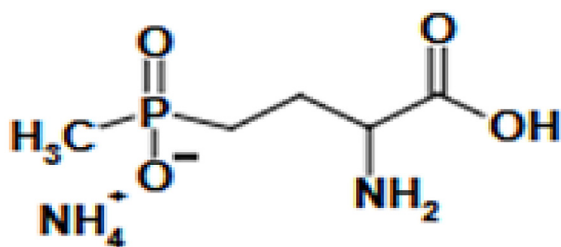


Figure 1. Molecular structure of glufosinate ammonium (Rosati, 2011)

The route of action of glufosinate has been debatable, and ammonia buildup has frequently been responsible for its quick phytotoxicity. According to recent research, lipid peroxidation and the buildup of reactive oxygen species are the causes of the contact activity of glufosinate. Glufosinate causes photo reduction of molecular oxygen, which produces reactive oxygen species, by interfering with both photorespiration and the light reactions of photosynthesis.

Glufosinate ammonium functions by inhibiting glutamine synthetase an essential enzyme for the synthesis of glutamine in plants. This inhibition leads to the accumulation of ammonia, causing plant cell death. Glufosinate Ammonium acts by disrupting the glutamine synthetase enzyme in certain bacterial. This enzyme plays a crucial role in nitrogen metabolism, essential for bacterial growth and functioning.

The herbicides inhibitory effect can impact various bacterial populations involve in waste water treatment. These include the bacteria responsible for breaking down organic matter, nitrifying bacteria involved in ammonia removal, and denitrifying bacteria crucial for nitrogen removal (Chen *et al.*, 2020; Panpan *et al.*, 2014).

Wastewater treatment relies heavily on microbial activity to break down pollutants and organic matter. However, the presence of glufosinate ammonium can inhibit these microorganisms' ability to function effectively and negatively impacts aquatic organisms on (Vallejo *et al.*, 2018). Even though the pesticide was classified as “not likely to be a human carcinogen”, acute dietary exposure is of great concern for all crop harvests, livestock and humans having been linked to development of various health conditions such as endocrine disruption and neurological problems (Johnson and Sumpter, 2019).

Currently, glufosinate ammonium is included in the PAN International list of Highly Hazardous

Pesticides and banned in 29 countries mostly in Europe, however the product is much in use within Africa (Donthi and Kumar, 2022).

The alarming impact of glufosinate on aquatic ecosystems due to its persistence and slow degradation (Geng *et al.*, 2018) underscores the urgent need for effective remediation strategies. To manage the adverse effect of glufosinate ammonium, like other pesticides in the wastewater system, degradation mechanisms play a crucial role in reducing the concentration of herbicides. However, for glufosinate ammonium, biotic degradation by microorganisms suffers a setback as it undergoes microbial metabolism to form several metabolites like 3-(hydroxyl phosphinyl) propionic acid, which are more toxic than the original product (Masiol *et al.*, 2018; Takano and Dayan, 2020).

Unfortunately, membrane filtration techniques like reverse osmosis which seem effective in removing glufosinate, also suffers high cost implication. Likewise, advanced oxidation processes, utilizing strong oxidants like hydroxyl radicals – even though expensive– offer another avenue for Glufosinate degradation, potentially destroying it into harmless by products (Chen *et al.*, 2020).

This necessitated the search into a low cost strategy such as adsorptive removal of the product without the need for the degradation of glufosinate ammonium into a more harmful by products. Also, adsorption onto activated carbon or biochar has emerged as a promising approach, offering removal with high capacities (Wang *et al.*, 2023).

In order to optimize the adsorptive process, the design of experiment (DoE) approach is used by response surface methodology (RSM) to gather data and point out important variables and interactions that affect the process response. A mathematical model that captures the sporadic interactions between factors and responses is also developed using RSM to optimize the casualty model as the objective function in order to obtain optimal factor settings (Liu and Cherg, 2024).

This approach, which is widely used for process optimization, is effective in the settings where engineers have total control over the levels and treatments of factors, such as in computer experiments, scientific method applications, laboratory experiments, and any other research settings where controllable factors are present. RSM gives engineers a way to determine the ideal parameter values for certain industrial processes or design improvement in order to maximize process/product attributes. RSM can ideally function based on

experimentation activities as long as engineers have the opportunity to set the process or equipment parameter.

Nowadays, process optimization is crucial in all industries to determine the ideal operating parameters, produce better outcomes, as well as save money and production time (Liu and Cherg, 2024).

Many researchers and engineers around the world have become interested in the intriguing variety of RSM applications in recent years. Several engineering physical processes have been modeled, simulated, and optimized using RSM, a statistical technique, and artificial neural networks (ANN), a soft computing technology. It is also a statistical tool for determining the best combination of process variables for the development of a system or product. It looks at the effects of a few selected independent variables that are taken into consideration in the research on response variables of interest (Ishiwu, 2022).

The aim of this study is to develop an efficient and low cost adsorptive material from rice husk and clay (briquette) and adopt RSM to optimize the removal efficiency of glufosinate ammonium from wastewater.

MATERIALS AND METHODS

Sampling

Briquettes were produced mainly from rice husk and clay, while rice husk were obtained from the rice milling factory (7°85'1738N and 9°66'7455E), the clay was excavated at Federal University Wukari (7°82'4075N and 9°75'6354E) both in Wukari local Government area Taraba State. A non-selective herbicide with the name

Dragon super a product of Wacot Nigeria limited (Batch Number: 20240501 NAFDAC Reg Number: A10-100285) with active ingredient glufosinate ammonium was used as adsorbate. Dragon super was purchased from Agro Chemical firm (NICOL) at Wukari, Nigeria.

Distilled water for the preparation of stock of glufosinate ammonium was obtained from central laboratory FUW, HCl and NaOH used were of analytical grade and were obtained sigma Aldrich.

Preparation of carbonized rice husk-clay blend briquettes

Carbonized rice husk-clay blend briquette was prepared as described by Suryaningsih *et al.* (2018) using rice husk, clay, distilled water, crucible and drying tray. The rice husk obtained from a rice mill was dried under room temperature over a period of 48 hours. Afterwards, 400 g equivalent of the rice husk in crucibles were placed in a furnace and subjected heating at a temperature of 300 °C using furnace until the husk completely turns into carbon within 20 to 30 min. The carbonized rice husk produced was then transferred into a drying tray and cool for 30 minutes. Before weighing and adding approximately 200 g fine clay, mixed with 1.0 L of distilled water to the approximately 400 g of the carbonized rice husk and mixed thoroughly into paste. The paste formed was molded into shapes and air dried for 7 days to form the briquette before pulverizing. The product (adsorbent) were transferred into two different containers and one was labeled carbonized rice husk – clay blend briquette (CRHCB) before adsorption while the other was employed for the adsorptive studies and afterwards labeled carbonized rice husk – clay blend briquette (CRHCBA) after adsorption (Figure 2).

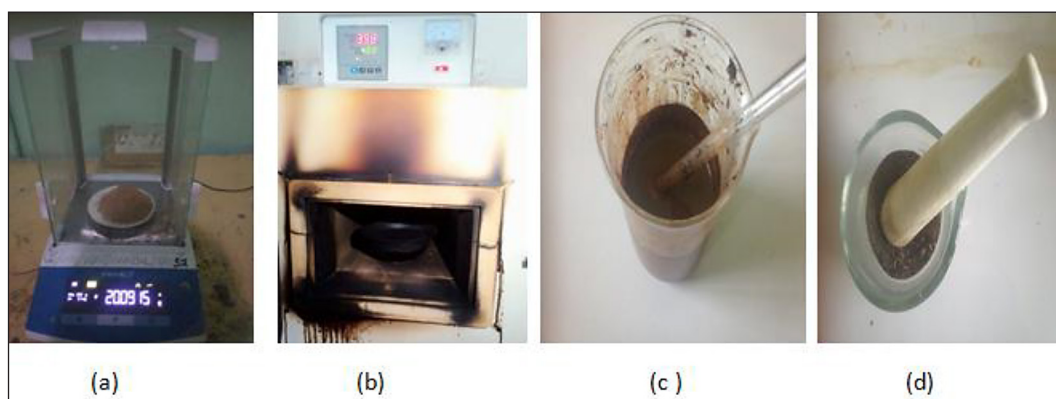


Figure 2. (a) Rice husk weighing, (b) rice husk carbonization, (c) rice husk-clay blending and (d) rice husk-clay blend pulverization

Adsorptive experimental design

The experiment was designed by means of Design-Expert (version 13), adopting response surface, design types: box-behnken and quadratic design model due to its ability *generate higher order response surfaces* using fewer required runs than a normal factorial technique.

The independent variables for the glufosinate ammonium removal process considered include: pH, temperature (°C), contact time (min) and adsorbent dosage of CRHCB (g) based on three levels coded as +1, 0, −1. The coded values of the independent variables X_i were calculated by utilizing Equation 1 (Hasanzadeh et al., 2020; Najafi and Rahimi, 2022).

$$X_i = \frac{\mathcal{E}_i - [\mathcal{E}_{Hi} + \mathcal{E}_{Li}]/2}{[\mathcal{E}_{Hi} - \mathcal{E}_{Li}]/2} \quad (1)$$

where: X_i is the coded values of independent variables. The high and low levels of independent criteria are \mathcal{E}_{Hi} and \mathcal{E}_{Li} respectively. Y is the dependent criterion equation of the quadratic model shown in Equation 2:

$$Y = \beta_0 + \sum_{i=1}^4 \beta_i X_i + \sum_{i=1}^4 \beta_{ii} X_i^2 + \sum_{i=1}^3 \sum_{j=2}^4 \beta_{ij} X_i X_j \quad (2)$$

where: the independent criteria are represented by X_i and X_j , the regression coefficient constant, linear, quadratic, and interaction in terms of β_0 , β_i , β_{ii} , and β_{ij} , respectively.

The level of Central Composite Design (CCD) experiments considering the four effective independent parameters for the removal of glufosinate ammonium by (CRHCB) adsorbent include: pH (3, 7.5 and 12); temperature (20, 50 and 80 °C); adsorbent dose (0.5, 1.25 and 2.0 g) and adsorption time (25, 62.5 and 100 min). A total of 29 experimental runs were randomly selected and recommended by the design expert as shown in Table 1.

Batch adsorptive removal of glufosinate ammonium from wastewater

Wastewater for the study was prepared by measuring 100 mL of out of the glufosinate ammonium stock purchase with the initial concentration 200 g/L, and was transferred into a volumetric flask with a capacity of 500 mL containing about 200 mL distilled water and stirred before more distilled water was added to 500 mL mark of the flask and was labelled wastewater.

To 50 mL of the dilute solution (wastewater) measured in a conical flask using a measuring cylinder, 0.5 g of CRHCB (adsorbent) was weighed and added to the flask based on the experimental design displayed in Table 1. The solution was mixed by means of a stirring rod, the solution is taken to the water bath set at 20 °C, following the design, likewise experimental pH was equally set at 7.5 with the aid of HCl (0.1M), NaOH (0.1M) and pH meter. The removal of glufosinate ammonium by CRHCB was done with the aid of ZD-2 cycling multipurpose vibrator set at 800 rpm within the contact time of 62.5 minutes before filtering as shown in Figure 3. The same procedure was replicated for the other 28 experiments based on the conditions displayed in Table 1 and the sample containers properly labelled following the design. The residual concentration of glufosinate ammonium in the 29 filtrates were determine using ultraviolet visible spectrophotometer while the adsorbent residue after adsorption was characterized and compared with the original adsorbent before the adsorption process.

Characterization of carbonized rice husk clay blend briquette before and after adsorption

The sample was placed onto the specimen stub and coated with platinum evaporative coating under high vacuum in order to examine the surface morphology of CRHCB before and after adsorption using the SEM (JSM 6701F (JOEL) and TEM spectrometer. The working distance was 15 mm, and the voltage was 15 kV (Minuti et al., 2023). The elemental constituent of the adsorbent was investigated using the EDX spectrometer (Khan et al., 2021). The functional groups in CRHCB (adsorbent) before and after adsorption were identified using the FTIR spectrometer *Agilent Technology* (Cary 630 model) in a single-bounce attenuated total reflectance (ATR) mode coupled to a deuterated triglycine sulfate (DTGS) detector. Approximately 1.0 mg of each sample was placed on the diamond ZnSe crystal plate, and investigated within an average of 32 scans and 4 cm^{−1} resolution, while the spectrum was obtained in a transmission mode for a wavenumber range of 650–4000 cm^{−1}. The IR spectra were established using the spectroscopic software Win-IR Pro Version 3.0 with a peak sensitivity 2 cm^{−1} (Jacob et al., 2024). The EDX spectrometer was employed to investigate the elemental makeup of the adsorbent (Khan et al., 2021).

Table 1. Design expert recommendations of experiment runs

Experimental run	Dosage (g)	pH	Temperature (°C)	Time (minutes)
1	0.5	7.5	20	62.5
2	0.5	12	50	62.5
3	0.5	7.5	50	100
4	0.5	3	50	62.5
5	0.5	7.5	50	25
6	0.5	7.5	80	62.5
7	1.25	7.5	80	25
8	1.25	12	20	62.5
9	1.25	7.5	50	62.5
10	1.25	7.5	80	100
11	1.25	7.5	20	100
12	1.25	7.5	50	62.5
13	1.25	12	80	62.5
14	1.25	12	50	100
15	1.25	3	50	100
16	1.25	3	20	62.5
17	1.25	3	50	25
18	1.25	3	80	62.5
19	1.25	7.5	20	25
20	1.25	12	50	25
21	1.25	7.5	50	62.5
22	1.25	7.5	50	62.5
23	1.25	7.5	50	62.5
24	2	7.5	50	100
25	2	7.5	50	25
26	2	7.5	80	62.5
27	2	3	50	62.5
28	2	7.5	20	62.5
29	2	12	50	62.5

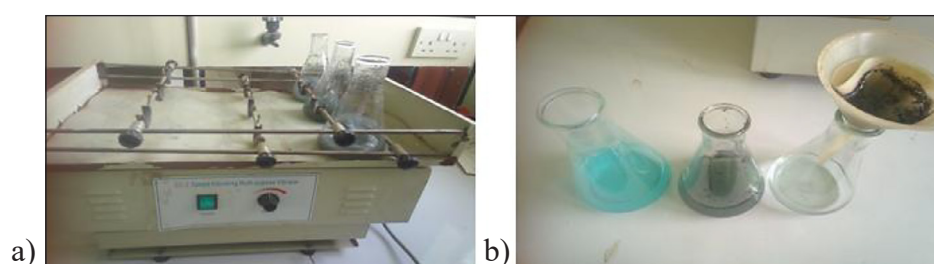


Figure 3. Adsorptive removal of glufosinate ammonium from wastewater: (a) glufosinate ammonium wastewater interaction with blended rice husk-clay briquette using ZD-2 cycling multipurpose vibrator (b) filtration after adsorption

Determination of residual concentration of glufosinate ammonium in the filtrate

The residual glufosinate content in the 29 experiments were estimated with the aid of UV-visible spectrophotometer (UV-6300PC

Spectrophotometer) set at 291 nm wavelength employing distilled water as blank. After obtaining calibration curve for the concentration versus absorbance of glufosinate ammonium using standard solutions of glufosinate ammonium at concentrations of 0, 0.5, 1, 1.5, and 2.0 g/L.

Data analyses

Equations 3 and 4 show the concentration difference between the starting concentration and the equilibrium concentration, which was used to compute the adsorption capacity (q_e) and adsorptive removal efficiency (R_e); where M is the mass of the adsorbent (rice husk briquette), V is the volume of the solution, R_e is the adsorptive removal efficiency, and C_o is the initial concentration of ammonium and C_e is the equilibrium concentration of ammonium (Seliem et al., 2013; Yerima and Donatus, 2023). The rate of glufosinate ammonium removal was estimated by dividing the amount of urea adsorbed by the respective contact time shown in equation V.

$$\text{Adsorption capacity } (q_e) = \frac{C_o - C_e}{M} \times V \quad (3)$$

$$\text{Removal efficiency } (R_e) = \frac{C_o - C_e}{C_o} \times 100 \quad (4)$$

$$\text{Rate of adsorption} = \frac{C_o - C_e}{t} \quad (5)$$

To evaluate the adsorption kinetics of glufosinate onto CRHCB, the pseudo-first order kinetic model and pseudo-second-order kinetic model were utilized as presented in the mathematical expressions 4 and V. K_1 and K_2 represents equilibrium rate constants (Ngouateu et al., 2015; Egah et al., 2019).

Pseudo-first order kinetic model:

$$\log(q_m - q_t) = \log q_m - \frac{k_1}{2.303} t \quad (6)$$

Pseudo-second order kinetic model:

$$\frac{t}{q_t} = \frac{1}{k_2 q_m^2} + \frac{1}{q_m} t \quad (7)$$

where: the values of K_1 and q_m are usually calculated from the plot of $\log(q_m - q_t)$ versus (t) which gives $\frac{k_1}{2.303}$ as slope and $\log q_e$ as intercept for the pseudo-first order kinetic model likewise for the pseudo second order, the kinetic constant k_2 and the theoretical q_m are obtainable from the plots of $(\frac{t}{q_t})$ versus (t) .

To further understand the adsorption behavior of glufosinate onto CRHCB, the Langmuir and Freundlich isotherm models were employed (Egah et al., 2019; Yerima et al., 2024).

Langmuir:

$$\frac{C_e}{q_e} = \frac{1}{K_L q_m} + \frac{C_e}{q_m} \quad (8)$$

A plot between C_e/q_e versus C_e will generate a straight line with a slope of $1/q_m$ and an intercept equals to $1/K_L q_m$.

The Langmuir isotherm behavior was investigated using separation factor (R_L) a dimensionless constant displayed in equation IX.

Separation factor:

$$\frac{1}{(1 + K_L C_o)} \quad (9)$$

where: the initial adsorbate concentration is C_o (mg/L), and the Langmuir constant for the adsorbate-adsorbent is K_L (L/mg). $R_L > 1$ indicates unfavorable adsorption, $R_L = 1$ indicates linear adsorption, R_L between 0 and 1 indicates favorable adsorption, and $R_L = 0$ indicates irreversible adsorption.

Freundlich:

$$\text{Freundlich: } \log q_e = \log K_F + \frac{1}{n} \log C_e \quad (10)$$

A plot of $\log q_e$ versus $\log C_e$ produces a straight line with a slope = $1/n$ and intercept = $\log K_F$.

RESULTS AND DISCUSSION

Characterization of the adsorbent

Scanning electron micrograph for surface morphological evaluation of rice husk briquette at 50 μ m magnifications displayed in Figure 4 shows the presence of pores with circular holes which are more visible before the adsorption than after. The reduction in visibility of these pores indicates adhesion of adsorbates to rice husk briquette surface after adsorption. The presence of active pores on adsorbent enhances adsorption.

Transmission electron microscope (TEM)

The transmission electron micrograph of the rice husk briquette at 50 nm reveals the presence of few measurable particles within the range of 2.70 nm to 6.37 nm which were spherical in shape and well disperse after adsorption. The presence of measurable particles at the surface suggests adsorption of particles on the surface of the adsorbent demonstrated in Figure 5.

Energy dispersive x-ray analysis (EDX)

The energy dispersive X-ray spectrum for CRHCB adsorbent revealed the presence of C, O,

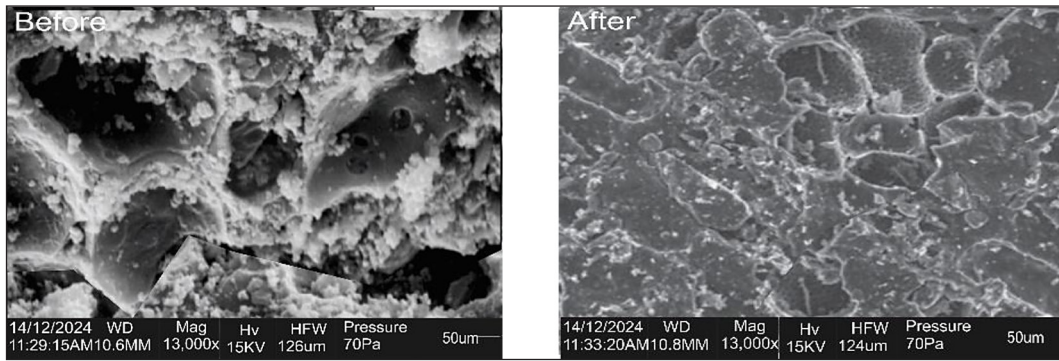


Figure 4. Scanning electron micrograph of rice husk-clay briquette before and after adsorption

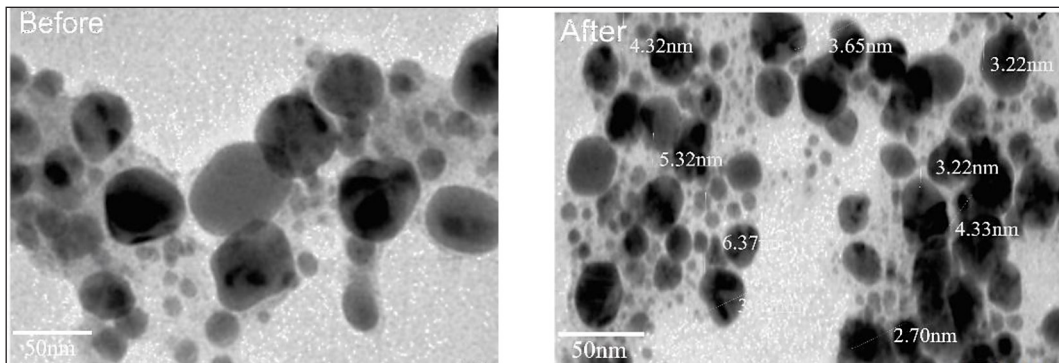


Figure 5. Transmission electron micrograph of rice husk-clay blend adsorbent before and after glufosinate adsorption at 50 nm

K, Si, Ca, Mg, Al, Fe, and Cu in Figure 6. The percentage elemental composition by weight after adsorption was in the order: C (60.20%) > O (20.10%) > Cu (5.00%) > Ca (4.23%) > Fe (3.10%) > Si (2.17%) > K (1.20%) = Al (1.20). In turn, before adsorption, the percentage elemental composition by weight was in the order: C (57.45%) > O (20.30%) > Si (10.20%) > Ca (7.33%) > K (2.17%) > Al (1.30%) > Mg (1.25%). Despite the introduction of new elements like Fe and Cu due

to their presence in trace amount in the herbicide, there was an increase in the percentage composition of carbon being the main precursor of the adsorbate after adsorption.

The FTIR spectrum of rice husk briquette presented in Figure 7 indicates the presence of C, H and O interacting to form different bonds which may be single, double or triple in nature, capable of playing roles influencing surface chemistry and consequently adsorption of adsorbates.

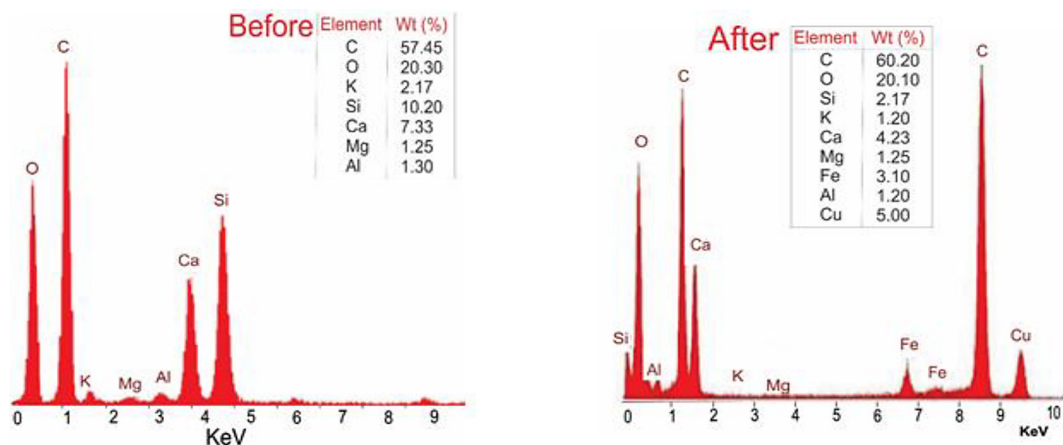


Figure 6. EDX spectrograph of rice husk-clay briquette before and after adsorption

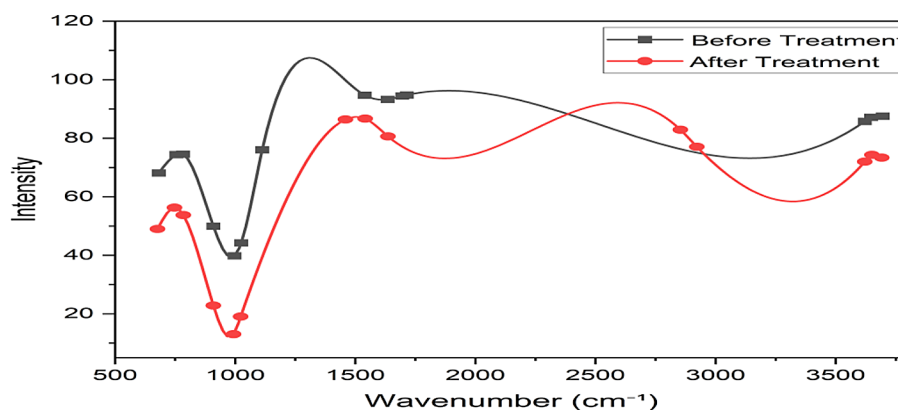


Figure 7. FTIR spectrum before and after glufosinate adsorption

A careful observation of the FTIR spectrum of the rice husk briquette before and after adsorption shows the presence of Si-O-Si and Al-OH bending around 950–750 cm^{-1} which is synonymous to clay mineral an additive of the adsorbent. Likewise, the presence of N-H bending vibration around 1650–1580 cm^{-1} and O-H vibrations of water molecules around 4000–3000 cm^{-1} . However, after glufosinate ammonium adsorption, addition bands were found around 1470–1450 cm^{-1} for C-H bend and 1541.3 cm^{-1} for N-O asymmetric stretch which are synonymous to groups associated with glufosinate ammonium indicating interaction between the adsorbent and the adsorbate.

There was an observable shift in wavenumber of CRHCB adsorbent before and after adsorption, thereby indicating a change in the vibrational frequency of a specific bond or functional group within the molecule, due to factors such as a change in bond strength, changes in the surrounding molecular environment. The various changes observed in the spectrum before and after adsorption is an indication of effective surface interaction between the adsorbate and the adsorbent during the adsorption process (Kibami *et al.*, 2014).

Adsorption capacity and removal efficiency

The adsorption capacity, removal efficiency and adsorptive rate of glufosinate ammonium after the adsorption process of the 29 experimental runs are displayed in Table 2. The result records an optimal removal efficiency of 90% for glufosinate ammonium with the corresponding adsorption capacity of 0.009 g/L and rate of 0.009 g/L. min^{-1} . This was achieved at pH 7.5, temperature of 20 °C, CRHCB dose of 1.25 g over a contact time of 100 mins. However, this was much greater

than the 10.14% optimal removal of glufosinate by means of carbonized ginger lily within the optimum condition (pH = 6, Temp. = 40 °C, Adsorbent dose = 1.0 g, Time = 60 mins) (Yerima *et al.*, 2025) but less than the 94.9% removal by means of electrosorption (Tongur and Ayranci, 2023).

Adsorption kinetics for the adsorption of glufosinate ammonium

To understand the kinetics of glufosinate ammonium adsorption onto CRHCB adsorbent under optimum conditions (pH 7.5, temperature of 20 °C and CRHCB dose of 1.25 g), the parameters were fitted into the pseudo first order and second order kinetics model over a contact time of 20, 40, 60, 80 and 100 mins, displayed on the kinetic plots in Figures 8 and 9, while the kinetic data are presented in Table 3. The pseudo first order kinetics was recorded at the rate $K_1(\text{min}^{-1})$ 0.4120, with regression coefficient $R^2 = 0.9226$ while the second order kinetic proceeds at the rate constant $K_2(\text{min}^{-1})$ 0.2243, with regression coefficient $R^2 = 0.9946$. On the basis of the higher value of R^2 , pseudo second order best describes the adsorption process of glufosinate ammonium indicating a chemisorption mechanism (Perez *et al.*, 2020).

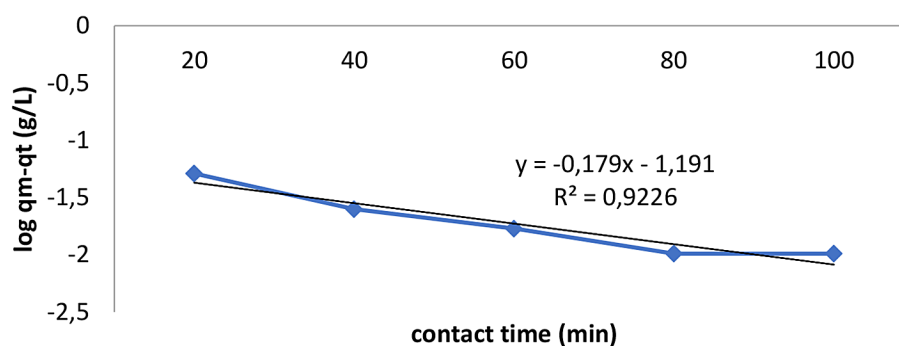
Adsorption isotherms for the adsorption of glufosinate ammonium

The data in Table 4 and isotherm plots in Figures 10 and 11 for Freundlich and Langmuir isotherms for the adsorptive removal of glufosinate ammonium under optimum conditions revealed a correlation coefficient R^2 (0.9877) for Freundlich to be higher than that of Langmuir with correlation coefficient R^2 0.0714 implying that the adsorption

Table 2. Glufosinate ammonium residual concentration and its removal efficiency

Exp. Runs	Dosage (g)	pH	Temp. °C	Time (min)	Co (g/L)	Ce (g/L)	Amount adsorbed (g/L)	Adsorption rate (g/L.min ⁻¹)	Qe (g/L)	Re (%)
1	0.5	7.5	20	62.5	1.0	0.64	0.36	0.0057	0.0036	36
2	0.5	12	50	62.5	1.0	0.88	0.12	0.0019	0.0019	12
3	0.5	7.5	50	100	1.0	0.8	0.2	0.0020	0.0020	20
4	0.5	3	50	62.5	1.0	0.88	0.12	0.0019	0.0019	12
5	0.5	7.5	50	25	1.0	0.68	0.32	0.0128	0.0128	32
6	0.5	7.5	80	62.5	1.0	0.94	0.06	0.0009	0.0009	6
7	1.25	7.5	80	25	1.0	0.49	0.51	0.0204	0.0240	51
8	1.25	12	20	62.5	1.0	0.9	0.1	0.0016	0.0016	10
9	1.25	7.5	50	62.5	1.0	0.52	0.48	0.0077	0.0048	48
10	1.25	7.5	80	100	1.0	0.8	0.2	0.0020	0.0030	20
11	1.25	7.5	20	100	1.0	0.1	0.9	0.0090	0.0090	90*
12	1.25	7.5	50	62.5	1.0	0.64	0.36	0.0058	0.0058	36
13	1.25	12	80	62.5	1.0	0.76	0.24	0.0038	0.0122	24
14	1.25	12	50	100	1.0	0.82	0.18	0.0018	0.0018	18
15	1.25	3	50	100	1.0	0.82	0.18	0.0018	0.0082	18
16	1.25	3	20	62.5	1.0	0.64	0.36	0.0058	0.0058	36
17	1.25	3	50	25	1.0	0.91	0.09	0.0036	0.0036	9
18	1.25	3	80	62.5	1.0	0.9	0.1	0.0016	0.0016	10
19	1.25	7.5	20	25	1.0	0.48	0.52	0.0208	0.0210	52
20	1.25	12	50	25	1.0	0.76	0.24	0.0096	0.0038	24
21	1.25	7.5	50	62.5	1.0	0.59	0.41	0.0066	0.0066	41
22	1.25	7.5	50	62.5	1.0	0.58	0.42	0.0067	0.0067	42
23	1.25	7.5	50	62.5	1.0	0.7	0.3	0.0048	0.0048	30
24	2	7.5	50	100	1.0	0.52	0.48	0.0048	0.0048	48
25	2	7.5	50	25	1.0	0.4	0.6	0.0240	0.0200	60
26	2	7.5	80	62.5	1.0	0.5	0.5	0.0080	0.0080	50
27	2	3	50	62.5	1.0	0.5	0.5	0.0080	0.0080	50
28	2	7.5	20	62.5	1.0	0.54	0.46	0.0074	0.0074	46
29	2	12	50	62.5	1.0	0.9	0.1	0.0016	0.0016	10

Note: removal efficiency = Re, adsorption capacity = Qe, temperature = temp., initial concentration = Co, Equilibrium concentration = Ce.

**Figure 8.** Pseudo first order kinetics plot for glufosinate adsorption

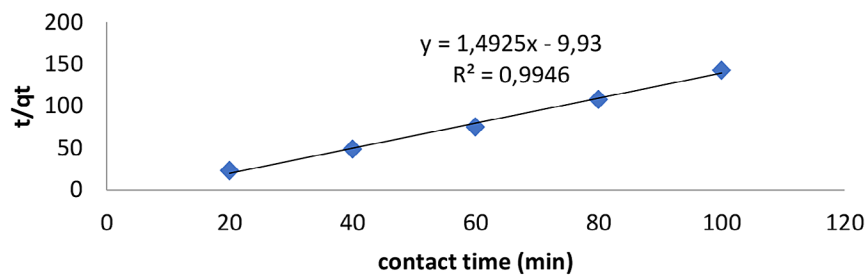


Figure 9. Second order kinetics plot for glufosinate adsorption

Table 3. Pseudo first and second order kinetic parameters for the adsorption of glufosinate

Model	Parameter	CRHCB
First order	K_1 (min^{-1})	-0.4120
	Q_e (mg/g)	0.0644
	R^2	0.9226
Second order	K_2 (min^{-1})	-0.2243
	Q_e (mg/g)	0.6700
	R^2	0.9946

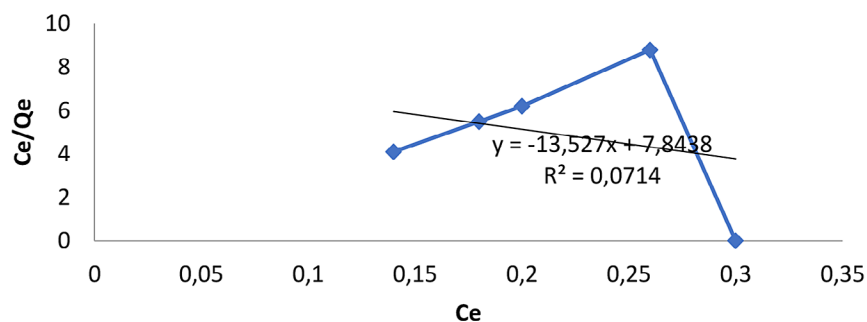


Figure 10. Langmuir isotherm plot for glufosinate adsorption

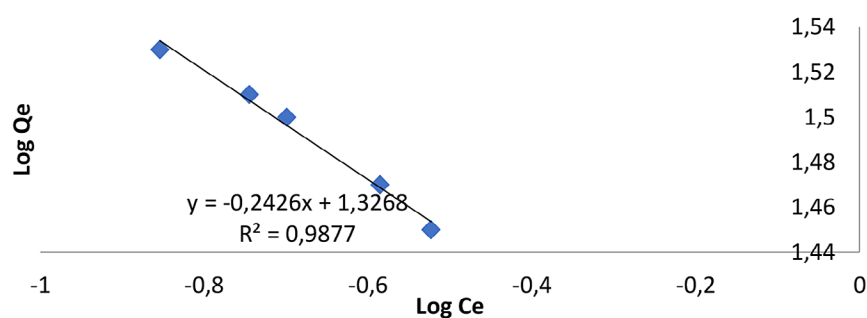


Figure 11. Fruendlich isotherm plot for glufosinate adsorption

Table 4. Isotherm parameters for the adsorption of glufosinate

Model	Parameters	CRHCB
Langmuir isotherm	Q_m (mg/mL)	-0.074
	K_L	-1.725
	R^2	0.0714
	R_L	-1.379
Freundlich isotherm	K_F	21.22
	R^2	0.9877
	$1/n$	-0.2426
	n_F	-4.122

Note: carbonized rice husk – clay blend = CRHCB.

of glufosinate ammonium is best explain with the Freundlich isotherms at the rate constant K_F of 21.22. Freundlich isotherm dominated mechanism shows that the adsorption is more heterogenous than homogenous (Jariani *et al.*, 2010).

CONCLUSIONS

This study revealed the potentials of carbonized rice husk-clay blended briquettes as a cost-effective, sustainable, eco-friendly and efficient adsorbent for the removal of glufosinate ammonium from wastewater. The FTIR spectrum reveals the presence of functional groups responsible for enhancing adsorbent- adsorbate surface interactions. The SEM and TEM confirm the presence of pore spacing in the adsorbent and the saturation of those spaces after the adsorption process. EDX analysis of the adsorbent showed increment in percentage C the main precursor of glufosinate. The removal efficiency of 90% was achieved within the optimum condition (pH of 7.5, temperature, 20 °C, adsorbent dose of 1.25 g and contact time of 100 mins) at the rate of 0.009 g/Lmin⁻¹ following the pseudo second order kinetics and Freundlich isotherm. Conclusively, this study contributes to the growing body of knowledge on sustainable remediation of glufosinate from wastewater.

REFERENCES

- Chen, J., Guo, H., Lu, D., Lu, Y., Fu, H., Yuan, X. (2020). The degradation and transformation of glufosinate ammonium in a municipal sewage treatment plant. *Water Research*, 170, 115348.
- Donthi, N.R., Kumar, A.D.D (2022). *Glufosinate ammonium an overview*. Pesticide Action Network, India. 1–27. https://pan-india.org/wp-content/uploads/2024/03/Glufosinate-Ammonium-An-overview_PAN-India_Dec2022.pdf
- Egah, G.O., Hikon, B.N., Sheckhar, N.G. Yerima, E.A., Omovo, M., Aminu, F.A. (2019). Synergistic study of hydroxyiron (III) and kaolinite composite for the adsorptive removal of phenol and cadmium. *International Journal of Environmental Chemistry*, 3(1), 30–42.
- Geng, Y., Hu, C., Xu, M., Yang, Y., Wang, F. (2018). Adoption and degradation of glufosinate on different soils and sediments. *Ecotoxicology and Environmental Safety*, 150, 196–203.
- Hasanzadeh, M., Simchi, A., Far, H.S. (2020). *Nanoporous composites of activated carbon-metal organic frameworks* for organic dye adsorption. *Journal of Industrial Engineering and Chemistry*, 81, 405–414. <https://doi.org/10.1016/j.jiec.2019.09.031>
- Ishiwu, C.N. (2022). Response surface methodology (RSM): Review of the practical approach in food science and technology research. *International Journal of Agriculture, Food and Biodiversity*, 1(1), 52–59.
- Jacob, A.G., Musa, I., and Ogbesejana, A.B. (2024). Extraction, fir and gc-ms characterization of palm kernel oil for laundry soap production. *Scientia Africana*, 23(3), 185–196. <https://dx.doi.org/10.4314/sa.v23i3.18>
- Jariani, S.M.J., Rosenani, A.B., Samsuri, A.W., Shukor, A.J., and Ainie, H.K (2010). Adsorption and desorption of glufosinate ammonium in soils cultivated with oil palm in Malaysia. *Malaysian Journal of Soil Science*, (14), 41–52
- Johnson, A. C. and Sumpter, J. (2019). Risks from chemicals in the environment: Right concerns and right actions? *British Medical Bulletin*, 131(1), 5–16.
- Johnson, T.M. (2020). Leaching potential glufosinate ammonium in agricultural fields. *Groundwater Monitoring and Remediation*, 40(3), 45–52.
- Khan, A., Khan, M.S., Hadi, F., Saddiq, G.A.N. (2021). Energy dispersive xray (EDX) fluorescence based analysis of heavy metals in marble powder paddy soil and rice (*Oryza sativa* L.) with potential health risks in district Malakand, Khyber Pakhtunkhwa Pakistan, 33(1), 301–316.
- Kibami, D., Pongener, C., Rao, K.S., Sinha, D. (2014). Preparation and characterization of activated carbon from *Fagopyrum esculentum* Moench by HNO₃ and H₃PO₄ chemical activation. *Der Chemica Sinica*, 5(4), 46–55.
- Liu, S., Cherg, H. (2024). Manufacturing and optimization in the process industry. *International Journal of Information Technology and Web Engineering*, 19(1), 1–20.
- Masiol, A., Vigani, M., Bennicelli, R., Galletti, G.C. (2018). Occurrence and behavior of glufosinate and its metabolites MPP in surface water bodies affected by agricultural runoff. *Chemosphere*, 199, 362–370.
- Miller, T.H., Jones, L.E. (2021). Assessing the biodegradability and toxicity of glufosinate ammonium degradation products. *Chemosphere*, 263, 128094
- Minuti, A.E., Labusca, L., Hrea, D.D., Stonain, G., Chriac, H., Lupu, N. (2023). A simple protocol for sample preparation for scanning electron microscopic imaging allows quick screening of nanomaterials adhering to cell surface. *International Journal of Molecular Sciences*, 24(1), 430. <https://doi.org/10.3390/ijms24010430>
- Najafi, M., Rahimi, R. (2022). Synthesis of novel Zr-MOF/Cloisite-30B nano-composite for anionic and cationic dye adsorption: Optimization by design expert, kinetic, thermodynamic, and adsorption study. *Journal of Inorganic and Organometallic*

- Polymers and Materials*, 33, 138–150. <https://doi.org/10.1007/s10904-022-02471-1>
18. Ngouateu, L.R.B., Sone, P.M.A., Nsami, N.J., Kouotou, D., Belibi, P.D., Mbadcam, K.J. (2015). Kinetics and equilibrium studies of the adsorption of phenol and methylene blue onto cola nutshell based activated carbon. *International Journal of Current Research Reviews*, 7(9), 1–9.
19. Panpan, M., Haiyan, P., Wenrong, H., Yuanyuan, S., Zheng, L. (2014). How to increase microbial degradation in constructed wetlands: Influencing factors and improvement measures. *Bioresource Technology*, 157, 316–326. <https://doi.org/10.1016/j.biortech.2014.01.095>
20. Perez, I.D., Anes, I.A., Junior, A.B.B., Espinosa, D.C.R. (2020). Comparative study of selective copper recovery techniques from nickel laterite leach waste towards a competitive sustainable extractive process. *Cleaner Engineering and Technology*, <https://doi.org/10.1016/j.clet.2020.100031>
21. Rosati, D. (2011). Determination of residues of glufosinate ammonium in/on kidney bean after spraying of AE F03986600SL18 K9 in the field in France (south) Netherland. *Bayer Crop Science Report*, 9, 2137.
22. Seliem, M.K., Komarneni, S., Byrne, T. (2013). Removal of perchlorate by synthetic organosilicas and organoclay: kinetics and isotherm studies. *Applied Clay Science*, 71, 21– 26.
23. Suryaningsih, S., Nurhial, O., Yuliah, Y., Salsabila, E. (2018). Fabrication and characterization of rice husk briquette. *American Institute of Physics Conference Proceedings* 1927, 030044. <https://doi.org/10.1063/1.5021237> <http://aip.scitation.org/toc/apc/1927/1>
24. Takano, H.K., Dayan, F.E. (2020). Glufosinate ammonium: A review of current state of knowledge. *Pest Management Science*, 76(12). <https://doi.org/10.1002/ps.5965>
25. Tongur, T., Ayranci, E. (2023). Investigation of the performance of activated carbon cloth to remove glyphosate, glufosinate, aminomethyl phosphonic acid and bialaphos from aqueous solutions by adsorption/electrosorption. *Environmental Monitoring and Assessment* 195, 814. <https://doi.org/10.1007/s10661-023-11395-3>
26. Ugrina, M., Milojkovic, J. (2024). Advance in wastewater treatment. *Energies*, 16(17), 1400. <https://doi.org/10.3390/en17061400>
27. Vallejo, B., Picazo, C., Orozco, H., Matallana, E., Aranda, A. (2018). Herbicide glufosinate inhibits yeast growth and extends longevity wine fermentation. *Scientific Reports*, 7(1), 12414. <https://doi.org/10.1038/s41598-017-12794.6>
28. Wang, B., Lan, J., Bo, C., Gong, B., Ou, J. (2023). Adsorption of heavy metal into biomass derived activated carbon: A review. *RSC Advances*, 13(7), 4275–4302. <https://doi.org/10.1039/d3ra07911a>
29. Yerima, E.A., Maaji, S.P., Abutu, D., Ataitiya, H., Ekirigwe, O., Johnson, S.N., Shem, A. (2024). Adoption of response surface methodology in the optimization of ammonia removal from aquaculture effluent using thermal activated and non-activated ball clay. *IOSR Journal Environmental science, Toxicology and Food Technology*, 18(2), 1–9. <https://doi.org/10.9790/2402-1802020109>
30. Yerima, E.A., Donatus, R.B. (2023). Adsorptive removal of phosphate from agricultural effluent using thermally and non-thermally activated sepiolite clay. *UMYU Scientifica*, 2(4), 136 – 144. <https://doi.org/10.56919/usci.2324.017>
31. Yerima, E.A., Percy, N.U., Edmund, L.O., Abutu, D. (2025). Adsorptive removal of glufosinate ammonium in wastewater using carbonized ginger lily (*Costus afer*) *Chemistry of the Total Environment*, <https://doi.org/10.52493/j.cote.2025.1.125>